AIMS Materials Science, 8(5): 823–835.
DOI: 10.3934/matersci.2021050
Received: 04 October 2021
Accepted: 11 November 2021
Published: 16 November 2021

http://www.aimspress.com/journal/Materials

Research article

Multi-functional organic field effect transistor based on a dual doped P3HT

Thomas Debesay[1], Sam-Shajing Sun[1,2,*] and Messaoud Bahoura[1,3]

[1] Center for Materials Research, Norfolk State University, 700 Park Avenue, Norfolk, VA 23504, USA
[2] Department of Chemistry, Norfolk State University, 700 Park Avenue, Norfolk, VA 23504, USA
[3] Engineering Department, Norfolk State University, 700 Park Avenue, Norfolk, VA 23504, USA

* **Correspondence:** Email: ssun@nsu.edu; Tel: +17578232993.

Abstract: A dual doped regio-regular poly(3-hexylthiophene-2,5-diyl) (P3HT) was investigated to develop a multi-functional organic field effect transistor (OFET). OFETs based on a pristine P3HT and a dual doped P3HT (P3HT:PCBM:I_2 blend) were fabricated to study the impact of doping on the electrical properties of the samples, and to examine the mechanism through which it amplified the output performance of the doped OFETs. A series of experimental techniques such as device electrical characterization, active layer surface analysis, and photon absorptivity measurements were conducted to quantitatively characterize the principal parameters that are susceptible to change as a result of doping. Topographic mapping revealed the expected doping-induced improvements in surface morphology, which could be associated with the ability of iodine to improve interdigitation between adjacent P3HT chains. Similarly, absorption spectra showed a 3 nm red-shift of the light absorbance spectrum of the doped samples compared to the undoped samples. The electrical conductivity of the samples was also examined at various conditions of temperature and light intensity, and the values obtained from the doped sample were approximately one order of magnitude higher compared to those of the undoped sample at room temperature, which explains the reason behind the higher output current drawn from the doped device compared to that of the undoped OFET. The explanation for this is two-fold, both PCBM and iodine promote the generation of free charge carriers, which increases the electrical conductivity of the active layer; and in addition to that, the improved P3HT main-chain interdigitation brought about by the introduction of iodine results in an increase in charge-carrier mobility, which also results in higher electrical conductivity. The findings of this study offers valuable information that could be instrumental in further advancing the future organic semiconductors based studies.

Keywords: semiconducting polymers; doping; charge generation; charger mobility; thin-film morphology; organic field effect transistors (OFETs); multi-functionality

1. Introduction

While the cutting-edge silicon-based electronic devices are advancing in an unprecedented fashion, the call for cost-effective, environmentally friendly, lightweight, and physically flexible electronic products has brought enormous attention to the semiconducting-polymer-based technology. Over the past few decades, semiconducting polymers have been the focus of a wide spectrum of advanced research to overcome their inherent drawbacks, in an effort to make them commercially available and competitive with their silicon-based counterparts [1–4]. These studies have, to a certain extent, narrowed down the gap in performance and applicability between the traditional inorganic semiconductors and organic semiconductors in a wide range of applications [5–8] such as thermoelectric systems, photovoltaics, screen displays, biosensors, etc., in which, some of those applications have been commercialized successfully [9].

Regio-regular poly(3-hexylthiophene-2,5-diyl) (P3HT), a p-type conjugated semiconducting polymer, is among the list of most frequently studied semiconducting polymers. It has been the subject of many studies for a variety of applications, both in its pristine and doped forms [10–12]. Although they follow different mechanisms, scientific studies have shown that doping organic semiconductors has the same outcome as doping inorganic semiconductors, improvement in electrical conductivity [13–15]. As such, studies done on P3HT for potential thermoelectric and photoelectric applications have shown a noticeable enhancement in device performance as a result of doping [5,16–18]. As illustrated in those articles, the doping-induced performance enhancements could be attributed to multiple contributing variables associated with the introduction of the doping species into the host polymer semiconductor.

We have previously reported preliminary data on a multi-functional OFET based on a dual-doped P3HT [19]. In that study, the active layer of the OFETs comprised of P3HT, simultaneously doped with [6,6]-Phenyl C71 butyric acid methyl ester (a mixture of isomers (PCBM)) and iodine (I_2) to enhance the targeted photoelectric and thermoelectric functionalities, respectively. We found that each dopant resulted in improved device performance in their respective functionalities, compared to the P3HT-based OFETs. Such performance enhancement could be attributed to multiple doping induced factors, which includes improved molecular structural alignment which would favor charge carrier mobility, or it could also be as a result of donor/acceptor interface facilitated free charge carrier generation, or maybe both factors could have come to effect simultaneously. It is very important to underline that the charge transfer that takes place at the donor-acceptor interfaces is driven by the energy offset between the frontier orbitals (HOMO/LUMO) of the host polymer (P3HT) and that of the dopants (PCBM and Iodine). It is through this process that the free charge carrier density is improved. Schematic representation of both the photoelectric and thermoelectric charge transfer mechanisms are depicted in Figure 1a,b, respectively.

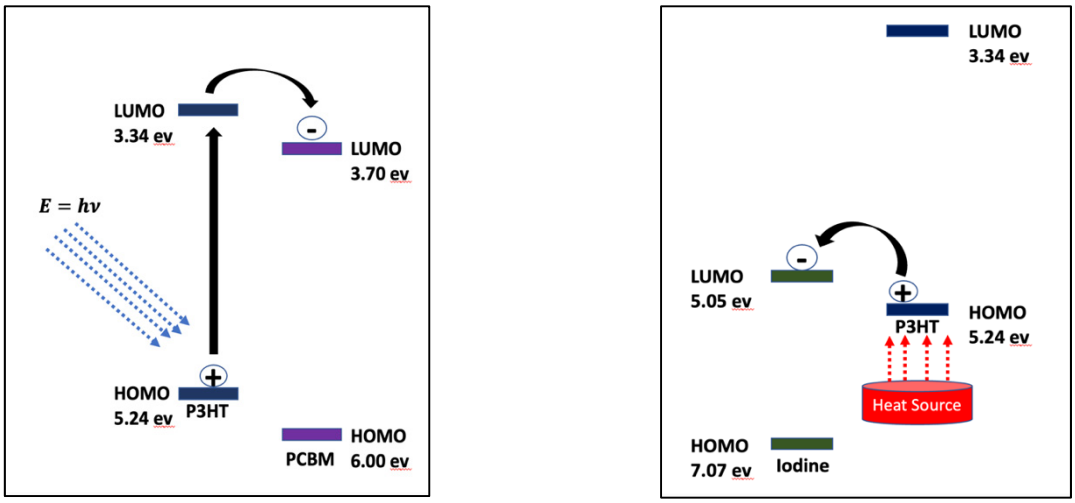

(a) (b)

Figure 1. (a) Schematic of a doping enhanced photoelectric (charge generation) process. (b) Schematic of a doping enhanced thermoelectric (charge generation) process.

In the present work, OFETs based on pristine-P3HT, and doped-P3HT were studied to investigate the impact of doping on the electrical properties of the doped samples, and the experimental results were analyzed to explain the doping-related performance enhancements seen in the doped OFETs. Additionally, it is worth mentioning that a great deal of optimization was done on the previously reported devices, that the data collected from these set of devices surpasses that the ones reported previously.

2. Materials and method

2.1. Device fabrication

Two types of organic semiconductor (OSC) solutions; one of P3HT (purchased from Sigma-Aldrich, product #: 445703), and one of a dual doped P3HT, were first prepared in two separate vials. The undoped solution was prepared by dissolving 10 mg of P3HT in 1 mL of 1,2-dichlorobenzene (purchased from Alfa Aeser, product #: A13881), while the doped solution was prepared by dissolving a mixture of 10 mg of P3HT, 0.5 mg of PCBM (purchased from Sigma-Aldrich, product #: 684465), and 0.5-mol% of iodine (purchased from Alfa Aeser, product #: A12278) in 1 mL of 1,2-dichlorobenzene. Both solutions were stirred with magnetic stirrer bars overnight. Every item consumed in this work was used as received from their respective vendors.

All the experimental measurements done in this work, except for the photo absorption studies, were conducted on organic field-effect transistor device samples. The OFETs were fabricated on prefabricated heavily doped n-type silicon wafers with an ~300 nm thick thermally grown SiO_2 dielectric layer. The steps of the device fabrication process are as follows: the wafers were first cleaned according to a series of standard cleaning procedures, which started with sonication in acetone and isopropyl alcohol baths for 10 min each, followed by 15 s of plasma cleaning. Following

the cleaning procedure, the wafers were subjected to a surface treatment process which was carried out by submerging the wafers in a 10 mM octyltrichlorosilane (OTS) solution for 20 min. After the dielectric layer surface modification process, the wafers were blow-dried with nitrogen gas, and then passed through another round of plasma cleaning for five seconds. Once the wafers have passed through the cleaning and surface treatment stages; the source, drain, and gate, gold (Au) contacts were deposited on the dielectric surface, where, a 3 nm thick chromium (Cr) film was first deposited to help the ~70 nm thick Au film adhere well to the dielectric surface. The metal contact deposition process was done inside a high-vacuum Electron-beam (E-beam) deposition chamber. A prefabricated source-drain deposition shadow mask with transistor channel length of 50 μm and channel width of 1 mm was used to transfer the patterns onto the dielectric surface. To complete the bottom-gate—bottom-contact thin-film transistor structural configuration (see Figure 2), the OSC solutions were spin-coated onto the top of the source-drain contacts at 1000 rpm for 30 s, followed by 3000 rpm for 10 s, covering the whole of the FET channel with a thin film of ~60 nm thickness. Finally, the OFETs were annealed inside a vacuum oven, at ~100 ℃, for 3 h.

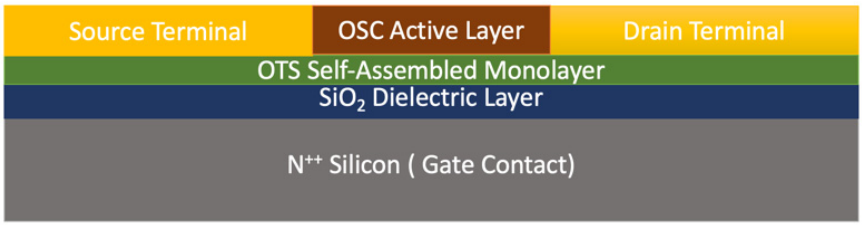

Figure 2. Schematic of the bottom-gate—bottom-contact structural configuration of the OFET.

For absorption studies, thin-films of the OSC solutions were spin-coated onto cleaned plain glass slides. Similar to the OFET samples, these samples were also annealed for 3 h inside a vacuum oven at ~100 ℃.

2.2. Characterization

The output current and transfer characteristics of the OFETs were measured using a KEITHLEY 4200-SCS semiconductor analyzer connected to a SIGNATONE 1160 series probe station. These measurements were carried out at varying conditions of light intensity and temperature. The impact of doping on the morphology (thin film surface topography) of the active layer was studied using a Bruker Veeco Dimension XT Atomic Force Microscope (AFM). As for the photo absorption measurements, the doped and undoped polymer films were measured by a PerkinElmer Lambda 1050 UV/VIS/NIR Spectrometer.

3. Results and discussion

As mentioned above, the OFETs were tested under varying conditions of light intensity and temperature. The doped sample's sensitivity to changes in light intensity and temperature, and its doping related improvements in performance, were analyzed by comparing to the performance produced by the undoped OFETs. The photoelectric measurements were carried out under light

intensities 2.22 mW/cm^2, 4.45 mW/cm^2, and 10.01 mW/cm^2; while the thermoelectric measurements were conducted at temperatures 20 ℃, 25 ℃, and 30 ℃. Each measurement was done at gate voltages +60 V, +30 V, 0 V, −30 V, and −60 V.

As indicated in the photoelectric output current performance of the OFETs shown in Figure 3, in both the doped and undoped devices, the increase in light intensity resulted in higher output current, and this is attributed to photoelectric mobile charge generation. However, if the performance of these device under the same test conditions is compared to each other, the doped devices outperformed the undoped samples by a significantly higher margin, ranging by as high as a factor of 30. This outcome is due to the presence of PCBM photo-acceptor in the doped samples, which led to more free charge carrier generation. Similarly, in the thermoelectric measurements, the thermoelectric effect in both the doped and undoped samples showed an increasing trend as the uniformly applied heat was increased. However, again, as shown in Figure 4, at each test temperature, the doped OFET produced higher output current than the undoped OFET. This is mainly attributed to the higher charge concentration (compared to the undoped samples) that resulted from the iodine thermoelectric dopant facilitated charge generation.

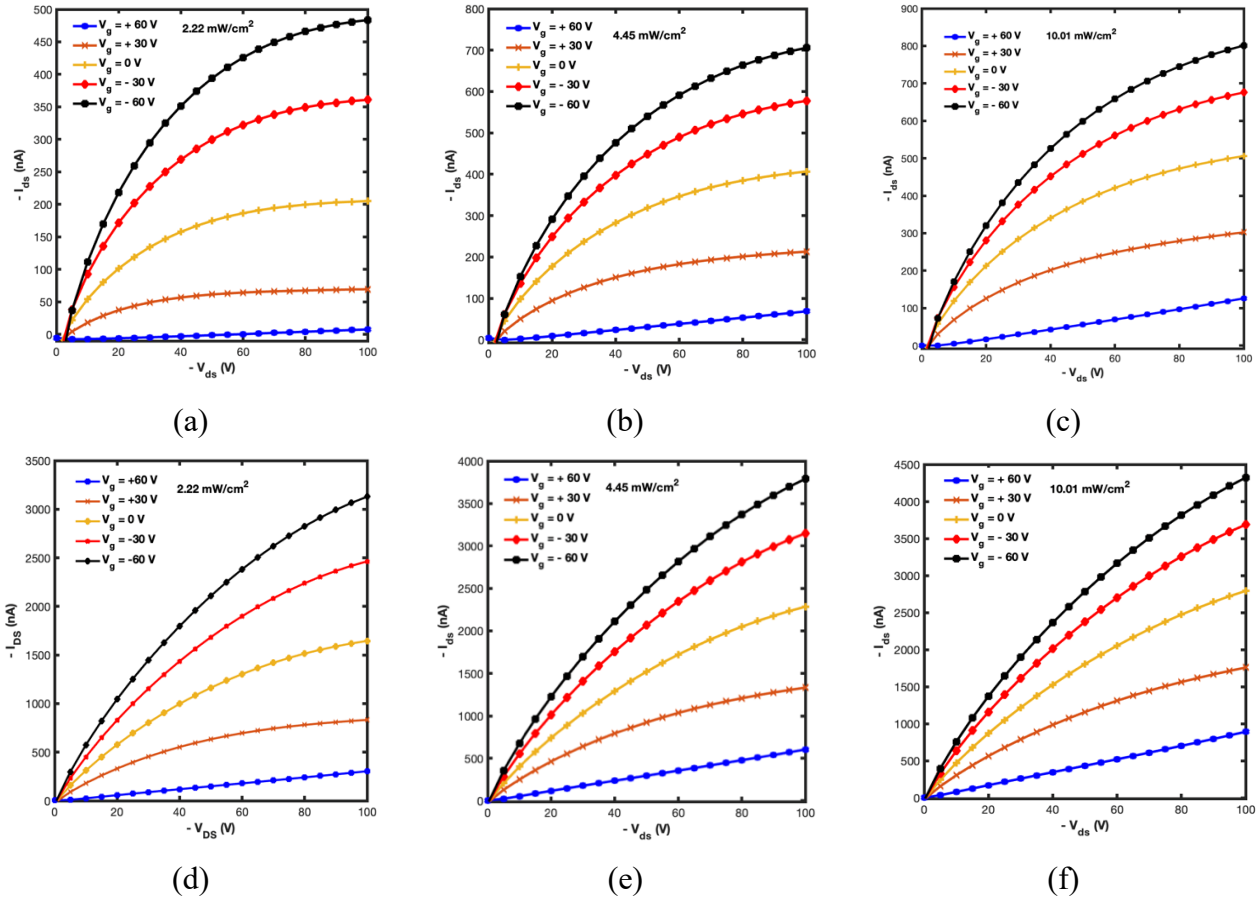

Figure 3. Source-drain output current I-V curves of the P3HT based OFET at (a) 2.22 mW/cm^2, (b) 4.45 mW/cm^2, and (c) 10.01 mW/cm^2. Source-drain output current I-V curves of the doped-P3HT based OFET at (d) 2.22 mW/cm^2, (e) 4.45 mW/cm^2, and (f) 10.01 mW/cm^2.

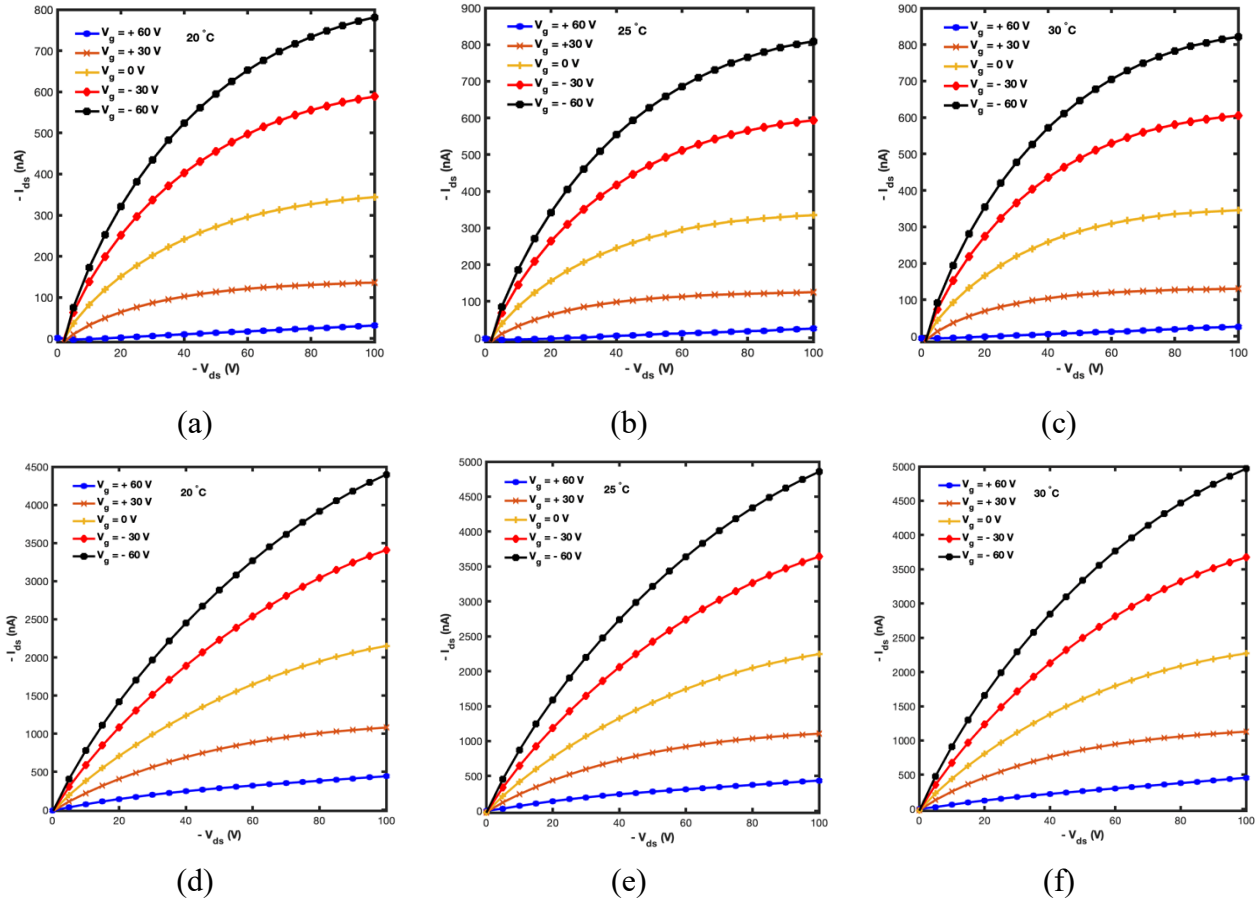

Figure 4. Source-drain output current I-V curves of the P3HT based OFET at (a) 20 °C; (b) 25 °C; and (c) 30 °C. Source-drain output current I-V curves of the doped-P3HT based OFET at (d) 20 °C; (e) 25 °C; and (f) 30 °C.

In our previous work, we concluded our findings with a hypothesis that the drastic increase in output current seen in the doped samples was as a result of doping induced improvement in the electrical conductivity (σ) of the active layer. To justify this hypothesis, in this work, we processed the far more optimized data acquired from both the doped and undoped samples, to quantitatively explain the impact of doping on the overall performance of the devices. The electrical conductivity of each sample, under each test condition, was calculated using the Ohmic model shown in Eq 1; where, "L" represents the transistor channel length, "A" represents the cross-sectional area of the gate voltage induced conducting channel, and "Ids" represents drain current at a particular drain voltage, "Vds". The values for Ids and Vds were extracted from the linear regime of the source-drain I-V curves acquired at Vg = −60 V. In a typical organic field effect transistor, the cross-sectional area of the conductive channel is determined by multiplying the channel width (W) by the thickness of the conductive channel (which has been reported to be in the range of 3.4–4 nm).

$$\sigma = \frac{I_{ds}\, L}{V_{ds}\, A} \tag{1}$$

In favor of the previously made assumption, the electrical conductivity plots in Figure 5a,b

show that each dopant resulted in enhancement of the electrical conductivity of the doped thin films, which ultimately resulted in better device performance of the doped OFETs compared to the undoped ones. Details on how much of an impact each dopant has in the much-improved performance exhibited by the dual-doped OFETs can be comprehended by weighing the effect of dual-doping covered in this study with the previously reported studies on only PCBM doped OFETs [20].

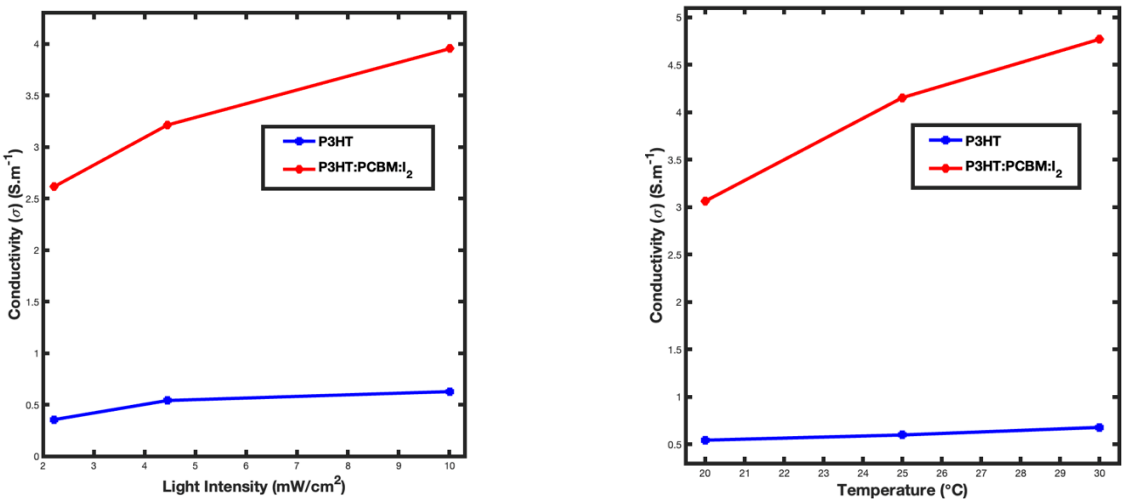

(a) (b)

Figure 5. Electrical conductivity of pristine and doped P3HT thin-film active layers plotted against (a) light intensity, and (b) temperature.

In the photoelectric measurements, the increase in electrical conductivity with light intensity is mainly attributed to the PCBM photo-acceptor facilitated Frenkel exciton dissociation into free charge carriers [21–24]. In addition to that, as has been reported previously [25], the introduction of iodine could have also resulted in the formation of new transitional states in the host P3HT molecules, leading to the generation of more free charge carriers from low-energy photons (visible light range). The latter effect was characterized using a UV-VIS-NIR spectrometer, and as shown in Figure 6, the light absorbance plot shows a red-shift of the absorption peak of the doped sample by ~3 nm. Furthermore, based on what has been reported in the literature, the higher electronegativity of iodine (2.66) compared to that of carbon (2.55) causes electrons to be transferred from the carbon atoms of the host P3HT main chain to the iodine dopant molecules, resulting in the formation of a C–I chemical bond, leaving the carbon atoms positively charged [26]. According to those reports, it is this C–I bond that enables the iodine doped samples to absorb light of longer wavelength (low energy) by promoting the formation of new optical transitions at lower energies than in the neutral P3HT, hence the red-shift. Another feature of iodine doping on facilitating exciton dissociation into free charge carriers was reported by Zhuo et al. [27]. In their report, they explained that this particular effect came about as a result of iodine inducing phase separation between P3HT and PCBM molecules. It is important to understand that, in terms of the overall impact of doping on the electrical conductivity of the doped samples, the imminent impact of iodine in generating free holes in the P3HT main chain via the C–I interaction goes hand-in-hand with the free charge carrier generation at the P3HT-PCBM and P3HT-I_2 interfaces. Therefore, we believe that those attributes

that are related to iodine could have played an indubitable role in the collective better outcome exhibited by the doped samples. The UV-Vis measurement was conducted in the wavelength range between 400–650 nm, with data point collection interval of 1 nm.

In the thermoelectric measurements, in addition to the thermoelectric charge generation (at the P3HT-I_2 interface), the increase in the electrical conductivity of the active layer with temperature, to a certain extent, can also be associated with the temperature-induced higher charge mobility.

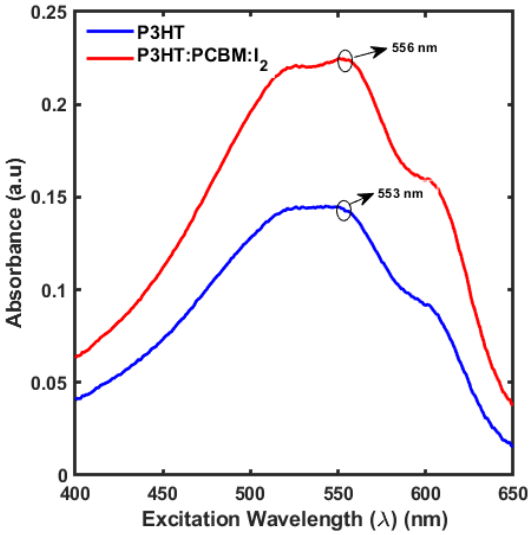

Figure 6. UV-Vis spectra of a pristine and a doped P3HT thin-films on plain glass substrates.

This doping related electrical conductivity enhancement was further evaluated from the standpoint of two important parameters that critically defines it, charge density and mobility.

The charge density analysis, in the conducting channels of the doped and undoped samples, was carried out to examine the impact of doping on charge carried density. The study was done at each test condition under which the electrical characterization of the OFETs was conducted, and as shown in the charge concentration plots shown in Figure 7, the charge density in the conducting channel of the doped sample was found to be higher than that of the undoped samples. The higher charge concentration (at each data point) observed in the doped sample is a clear indication that both the photoelectric and thermoelectric doping mechanisms effected their intended purpose, charge carrier generation. It is worth noting that the charge concentration indicated in the discussion is of the gate voltage induced conductive channel, not of the bulk of the active layer.

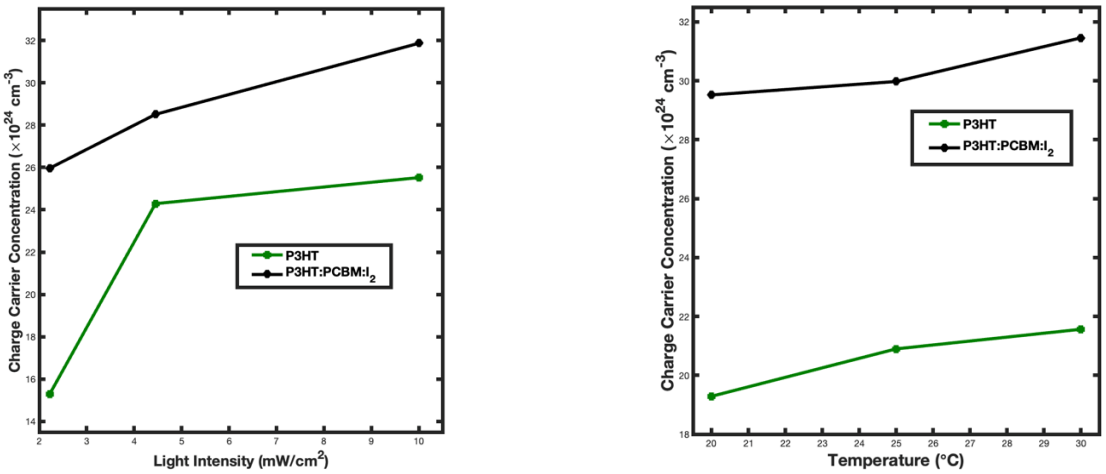

(a) (b)

Figure 7. Charge carrier concentration in the gate voltage induced conducting channels under varying conditions of (a) light intensity, and (b) temperature.

The principal purpose of the dual doping employed in this study was to enhance the ability of the P3HT-based OFETs to detect and respond to changes in light intensity and temperature. These effects were designed to come about as a result of the doping facilitated free charge carrier generation prompted improvement in the electrical conductivity of the active layer. With that being said, it is also important not to ignore the possibility of doping related morphological changes in the thin films. As proposed by Lee and Sun, iodine ions can stimulate improvement in P3HT main chain interdigitation (ordered main chain packing) [28]. Based off their claim, this more orderly packing leads to a structural arrangement on a molecular level; and based on that claim, one could hypothesize that the morphological enhancements would result in better charge carrier mobility in the polymer matrix. To examine if the low iodine doping concentration (0.5 mol%) used in this study has a meaningful impact on the thin-film active layer morphology, AFM scans were conducted on both the undoped and dual-doped samples. The surface roughness data shown in Figure 8a (as Roughness Average (R_a) and Root Mean Square (RMS) Roughness (R_q), elucidates that even at as low as 0.5 mol% doping concentration, iodine was effective in improving the surface morphology of the doped active layer. This observation falls in agreement with previously reported study on iodine doping [24], and based on those resemblances, here, we are making an assumption that the iodine doping could have also resulted in a more ordered P3HT chain packing, leading to higher charge transport. One way to experimentally warrant this assumption is to calculate charge mobility in the doped and undoped samples under the same test conditions and see if the results are in support of the argument. The linear charge-mobility (μ_{lin}) in the conducting channel of each device was calculated using Eq 2, where, "L" represents the channel length; "W" represents the channel width; "C_{ox}" represents the capacitance per unit area of the SiO_2 dielectric layer, and "V_d" represents the drain voltage at which the transfer characteristics measurements were conducted. The variables ∂I_{ds} and ∂V_{ds} were extracted from the linear regime of the transfer curves. As the data presented in Table 1 shows, under similar test conditions (at 20 ℃, 25 ℃, and 30 ℃), the charge mobility in the doped samples was higher than that of the undoped samples by approximately as high as a factor of 5. From

this observation, we can infer that the iodine doping-induced morphological improvement has, to a certain extent, elevated the performance of the doped devices by improving charge carrier mobility. Additionally, in both the doped and undoped samples, the increase in charge mobility with temperature adds to the overall contribution of mobility to the improved electrical conductivity with increase of temperature. The AFM images of the undoped and dual-doped P3HT thin films, from which the average surface roughness data was extracted from are displayed Figure 8b,c.

$$\mu_{lin} = \left(\frac{\partial I_{ds}}{\partial V_{ds}}\right) \frac{L}{W\, C_{ox}\, V_d} \tag{2}$$

Table 1. Charge carrier mobility in the undoped and doped P3HT based OFETs at temperatures 20 ℃, 25 ℃, and 30 ℃.

Temperature (℃)	Doped ($cm^2/V{\cdot}s$)	Undoped ($cm^2/V{\cdot}s$)
20	6.48×10^{-3}	1.76×10^{-3}
25	8.66×10^{-3}	1.79×10^{-3}
30	9.47×10^{-3}	1.97×10^{-3}

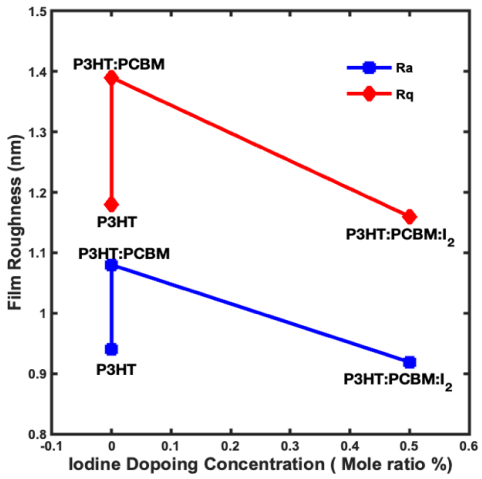

(a)

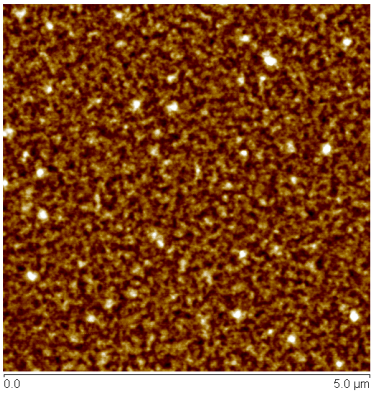

(b)

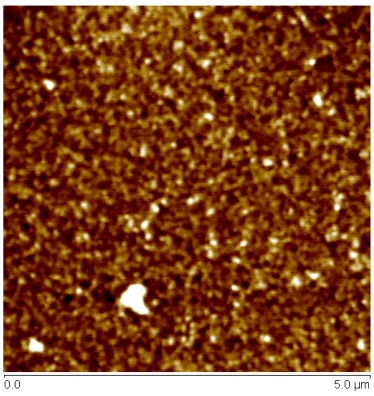

(c)

Figure 8. (a) Surface roughness (in terms of Ra and Rq) of the pristine and doped P3HT thin-films. (b) AFM image of a P3HT thin-film. (c) AFM image of a P3HT:PCBM:iodine blend (doped P3HT) based thin-film.

From a collective standpoint, all of the above-discussed doping-related attributes improved the electrical conductivity (σ) of the doped active layer by improving two critical parameters, carrier concentration (n) and mobility (μ); and this observation falls in agreement with Eq 3, which integrates the effect of charge density and charge mobility on the overall electrical conductivity of a semiconductor.

$$\sigma = ne\mu \tag{3}$$

4. Conclusion

In summary, OFETs with P3HT-based active layer were fabricated in both pristine and doped forms. The devices were characterized under varying temperature and light intensity test environments. The experimental data collected under those test conditions was analyzed to quantitatively characterize the electrical conductivity of both the undoped P3HT and dual-doped P3HT (P3HT:PCBM:I_2 blend) thin films. We found that the improvement in device performance seen in the doped samples was as result of doping induced enhancement in the electrical conductivity of the doped active layer. The electrical conductivity of the samples was then studied from different perspectives in relation to doping and doping-related parameters. Our findings showed that both the PCBM and iodine dopants contributed to the increase in charge density seen within the doped OFETs, while the iodine doping induced better interdigitation of the P3HT main chains resulted in a higher charge carrier mobility than that of the undoped OFETs. It is our supposition that the combination of these two effects is the driving force behind the much-improved device performance recorded from the doped OFETs. The findings of this study could be instrumental in further advancing future organic semiconductor based studies.

Acknowledgments

This research was supported by a center grant award from the US National Science Foundation (NSF Award #HRD-1547771).

Conflicts of interest

The authors declare no conflict of interest in this paper.

References

1. De Leeuw DM, Cantatore E (2008) Organic electronics: Materials, technology and circuit design developments enabling new applications. *Mat Sci Semicon Proc* 11: 199–204.
2. Huang J, Pfeiffer M, Werner A, et al. (2002) Low-voltage organic electroluminescent devices using pin structures. *Appl Phys Lett* 80: 139–141.
3. Lee YH, Jang M, Lee MY, et al. (2017) Flexible field-effect transistor-type sensors based on conjugated molecules. *Chem* 3: 724–763.
4. Facchetti A (2007) Semiconductors for organic transistors. *Mater Today* 10: 28–37.
5. Zhang Q, Sun Y, Xu W, et al. (2012) Thermoelectric energy from flexible P3HT films doped with a ferric salt of triflimide anions. *Energ Environ Sci* 5: 9639–9644.

6. Liu Z, Liu Q, Huang Y, et al. (2008) Organic photovoltaic devices based on a novel acceptor material: graphene. *Adv Mater* 20: 3924–3930.
7. Gelinck GH, Huitema HEA, Van Veenendaal E, et al. (2004) Flexible active-matrix displays and shift registers based on solution-processed organic transistors. *Nat Mater* 3: 106–110.
8. Lai S, Barbaro M, Bonfiglio A (2016) Tailoring the sensing performances of an OFET-based biosensor. *Sensor Actuat B-Chem* 233: 314–319.
9. Panasonic commercializes transparent OLED display module with superb image visibility. Available from: https://news.panasonic.com/global/press/data/2020/11/en201120-3/en201120-3.html.
10. Holliday S, Ashraf RS, Wadsworth A, et al. (2016) High-efficiency and air-stable P3HT-based polymer solar cells with a new non-fullerene acceptor. *Nat Commun* 7: 1–11.
11. Tiwari S, Singh AK, Joshi L, et al. (2012) Poly-3-hexylthiophene based organic field-effect transistor: Detection of low concentration of ammonia. *Sensor Actuat B-Chem* 171: 962–968.
12. Mun S, Park Y, Lee YEK, et al. (2017) Highly sensitive ammonia gas sensor based on single-crystal poly(3-hexylthiophene)(P3HT) organic field effect transistor. *Langmuir* 33: 13554–13560.
13. Yamamoto Y, Yoshino K, Inuishi Y (1979) Electrical properties of phthalocyanine-halogen complexes. *J Phys Soc Jpn* 47: 1887–1891.
14. Koopmans M, Leiviskä MA, Liu J, et al. (2020) Electrical conductivity of doped organic semiconductors limited by carrier-carrier interactions. *ACS Appl Mater Inter* 12: 56222–56230.
15. Liang Z, Zhang Y, Souri M, et al. (2018) Influence of dopant size and electron affinity on the electrical conductivity and thermoelectric properties of a series of conjugated polymers. *J Mater Chem A* 6: 16495–16505.
16. Zhang Y, Elawad M, Yu Z, et al. (2016) Enhanced performance of perovskite solar cells with P3HT hole-transporting materials via molecular p-type doping. *RSC Adv* 6: 108888–108895.
17. Lei X, Zhang F, Song T, et al. (2011) P-type doping effect on the performance of organic-inorganic hybrid solar cells. *Appl Phys Lett* 99: 267.
18. Lim E, Peterson KA, Su GM, et al. (2018) Thermoelectric properties of poly (3-hexylthiophene)(P3HT) doped with 2,3,5,6-Tetrafluoro-7,7,8,8-tetracyanoquinodimethane (F4TCNQ) by vapor-phase infiltration. *Chem Mater* 30: 998–1010.
19. Debesay TH, Sun SS, Bahoura M (2020) A polymer composite based organic FET multi-sensing device, *Organic and Hybrid Sensors and Bioelectronics XIII*, International Society for Optics and Photonics.
20. Debesay TH, Sun SS (2020) Phototransistors based on a lightly doped P3HT. *MRS Adv* 5: 1975–1982.
21. Aarnio H, Sehati P, Braun S, et al. (2011) Spontaneous charge transfer and dipole formation at the interface between P3HT and PCBM. *Adv Energ Mater* 1: 792–797.
22. D'Avino G, Mothy S, Muccioli L, et al. (2013) Energetics of electron-hole separation at P3HT/PCBM heterojunctions. *J Phys Chem C* 117: 12981–12990.
23. Clarke TM, Ballantyne AM, Nelson J, et al. (2008) Free energy control of charge photogeneration in polythiophene/fullerene solar cells: the influence of thermal annealing on P3HT/PCBM blends. *Adv Funct Mater* 18: 4029–4035.

24. Kniepert J, Lange I, Van Der Kaap NJ, et al. (2014) A conclusive view on charge generation, recombination, and extraction in as-prepared and annealed P3HT: PCBM blends: combined experimental and simulation work. *Adv Energ Mater* 4: 1301401.
25. Zhu H, Liu C, Song H, et al. (2014) Thermoelectric performance of poly(3-hexylthiophene) films doped by iodine vapor with promising high seebeck coefficient. *Electron Mater Lett* 10: 427–431.
26. Tian P, Tang L, Xiang J, et al. (2016) Solution processable high-performance infrared organic photodetector by iodine doping. *RSC Adv* 6: 45166–45171.
27. Zhuo Z, Zhang F, Wang J, et al. (2011) Efficiency improvement of polymer solar cells by iodine doping. *Solid State Electron* 63: 83–88.
28. Lee III HO, Sun SS (2018) Properties and mechanisms of iodine doped of P3HT and P3HT/PCBM composites. *AIMS Materi Sci* 5: 479–493.

AIMS Press